

Supported by



Accepted Article

Title: Efficient synthesis of D-phenylalanine from L-phenylalanine via a tri-enzymatic cascade pathway

Authors: Lu Cui, Zhang Sheng, Song Wei, Chen Xiulai, Liu Jia, Liu Liming, and Wu Jing

This manuscript has been accepted after peer review and appears as an Accepted Article online prior to editing, proofing, and formal publication of the final Version of Record (VoR). This work is currently citable by using the Digital Object Identifier (DOI) given below. The VoR will be published online in Early View as soon as possible and may be different to this Accepted Article as a result of editing. Readers should obtain the VoR from the journal website shown below when it is published to ensure accuracy of information. The authors are responsible for the content of this Accepted Article.

To be cited as: *ChemCatChem* 10.1002/cctc.202100237

Link to VoR: <https://doi.org/10.1002/cctc.202100237>

FULL PAPER

Efficient synthesis of D-phenylalanine from L-phenylalanine via a tri-enzymatic cascade pathway

Cui Lu,^[a,b] Sheng Zhang,^[c] Wei Song,^[a,b] Jia Liu,^[b] Xiulai Chen,^[b] Liming Liu,^[b] and Jing Wu*^[a]

Abstract: D-phenylalanine is an important intermediate in the food and pharmaceutical industry. Here, to enable efficient D-phenylalanine biosynthesis from L-phenylalanine, a tri-enzymatic cascade was designed and reconstructed *in vivo*. The activity of *Proteus vulgaris* meso-diaminopimelate dehydrogenase (PvDAPDH) toward phenylpyruvic acid was identified as the limiting step. To overcome the tension in the phenylpyruvic acid side-chain, PvDAPDH was engineered, generating PvDAPDH^{W121A/R181S/H227I}, whose catalytic activity of 6.86 U mg⁻¹ represented an 85-fold increase over PvDAPDH. Introduction of PvDAPDH^{W121A/R181S/H227I}, *P. mirabilis* L-amino acid deaminase, and *Bacillus megaterium* glucose dehydrogenase in *E. coli* enabled the production of 57.8 g L⁻¹ D-phenylalanine in 30 h, the highest titer to date using 60 g L⁻¹ L-phenylalanine as starting substrate, which meant a 96.3% conversion rate and >99% enantioselectivity on a 3-L scale. The proposed tri-enzymatic cascade provides a novel potential bio-based approach for industrial production of D-phenylalanine from cheap amino acids.

Introduction

D-phenylalanine (D-Phe), a non-protein amino acid, is used as a building block for pharmaceuticals and fine chemicals^[1]. Currently, D-Phe is produced mainly via enzymatic methods^[2], including (i) hydantoinase processes^[3], (ii) transamination^[4], (iii) resolution of racemate^[5], and (iv) reductive amination. The latter, which is catalyzed by meso-diaminopimelate dehydrogenase (DAPDH, EC 1.4.1.16), has the greatest potential^[6] as it can convert phenylpyruvic acid (PPA) and NH₄Cl to D-Phe in a single step with high enantioselectivity.

DAPDH, an NADP⁺-dependent oxidoreductase^[7], catalyzes the reversible oxidative deamination of meso-diaminopimelate (meso-DAP) in the D-center and stereoselective reductive amination from the corresponding α -keto acid^[8]. Based on substrate specificity and structural characteristics^[9], DAPDH can be divided in two classes. Type I, represented by

Corynebacterium glutamicum CgDAPDH^[10], is approximately 327 amino acids (aa) in length and shows high selectivity for meso-DAP^[9]. Type II, represented by *Symbiobacterium thermophilum* StDAPDH^[11], encompasses an average of 299 aa and accepts a wide range of substrates, including meso-DAP and other D-amino acids^[9, 12]. However, the narrow substrate spectrum of type I and the lower catalysis rate of type II DAPDHs often limit the industrial production of D-amino acids. Therefore, structure-guided engineering of the binding pocket and random mutagenesis have been applied to broaden the substrate spectrum or improve catalytic efficiency. For example, mutating residues R196, T171, H245, Q151, and D155 in CgDAPDH to R196M, T171I, H245N, Q151L, and D155G yielded the variant CgDAPDH^{BC621}, whose substrate range also included aliphatic and aromatic amino acids^[6]. Similarly, structure-guided site-saturation mutagenesis in the pocket of StDAPDH yielded StDAPDH^{W121L/H227I}, which displayed dramatically improved catalytic activity toward bulky 2-keto acids, such as PPA (70-fold) and 2-oxo-4-phenylbutyric acid (34-fold)^[13]. As NADPH serves as a hydrogen donor during DAPDH-mediated catalysis, cofactor recycling by glucose dehydrogenase (GDH)^[14] or formate dehydrogenase (FDH)^[15] is required. Hence, one of the protein engineering strategies employed to DAPDH was to change cofactor preference from NADPH to NADH. Accordingly, introduction of R35S/R36V/Y76I mutations in StDAPDH increased the NAD⁺/NADP activity ratio from 0.13 to 1.39^[16].

In this study, an artificial enzymatic cascade capable of converting L-Phe to D-Phe was designed and reconstructed *in vivo*. A “tension release” strategy affecting the substrate side-chain was developed to improve the catalytic efficiency of PvDAPDH toward PPA and increase D-Phe titers. Finally, by integrating the best catalytic variant, PvDAPDH^{W121A/R181S/H227I}, into the cascade, 57.8 g L⁻¹ D-Phe was synthesized with 96.3% conversion and >99% enantiomeric excess (ee) within 30 h in a 3-L fermentor.

Results

Design and *in vitro* reconstruction of a tri-enzymatic cascade for D-Phe synthesis

As illustrated in Figure 1a, D-Phe synthesis from L-phenylalanine (L-Phe) occurs in two steps: first, L-Phe undergoes oxidative deamination by L-amino acid deaminase (LAAD, EC 1.4.3.2) to produce the prochiral intermediate PPA; second, PPA undergoes reductive amination by DAPDH to generate D-Phe, with GDH (EC 1.1.1.47) coupling to regenerate NADPH. To reconstruct the cascade pathway *in vitro*, *Proteus vulgaris* PvDAPDH (Table S1), *P. mirabilis* PmLAAD variant, and *Bacillus megaterium* BmGDH^[17] were selected based on their specific enzymatic activities. The

[a] C. Lu, W. Song, Prof. J. Wu
School of Pharmaceutical Science
Jiangnan University
Wuxi 214122, China
E-mail: wujing@jiangnan.edu.cn

[b] C. Lu, W. Song, J. Liu, X. Chen, Prof. L. Liu
State Key Laboratory of Food Science and Technology
Jiangnan University
Wuxi 214122, China

[c] S. Zhang
Tianrui Chemical Co., Ltd
Department of Chemistry
Quzhou 324400, China

FULL PAPER

three selected genes were amplified, overexpressed, and purified (Figure S1, Table S2). To assess the feasibility of the proposed in vitro reconstruction system, the three enzymes were combined in an equimolar ratio and reacted with 5 g L⁻¹ L-Phe, 0.5 mM NADP⁺, 1 g L⁻¹ NH₄Cl, and 7 g L⁻¹ glucose for 4 h, after which 1.2 ± 0.1 g L⁻¹ D-Phe was detected (Figure S3). The identity of the final product was confirmed using mass spectrometry and NMR analysis (Figure S5-7). This result demonstrated that the designed cascade composed of PvDAPDH, PmLAAD, and BmGDH successfully converted L-Phe to D-Phe.

The effect of altering the BmGDH:PvDAPDH activity ratio (from 0.1:1 to 3:1) was investigated with 20 g L⁻¹ PPA and DAPDH activity fixed at 4 U mL⁻¹. As illustrated in Figure 1b, when the BmGDH:PvDAPDH activity ratio reached 0.3:1, the D-Phe titer stabilized at 18.5 ± 0.4 g L⁻¹, with 92.7% conversion rate. Similarly, when the PmLAAD:PvDAPDH activity ratio was set to 0.6–1.0:1, the D-Phe titer was 16.5 ± 0.4 g L⁻¹, with 82.7% conversion rate (Figure 1c). Therefore, the optimum PmLAAD:PvDAPDH:BmGDH activity ratio was set to 0.6–1.0:1:0.3.

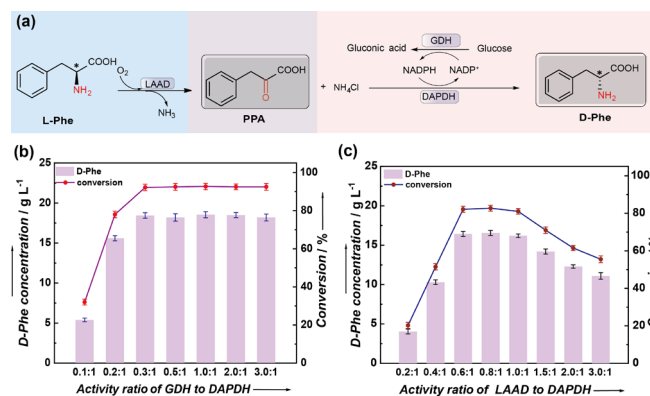


Figure 1. D-Phe biosynthesis pathway starting from L-Phe; (a) Designed D-Phe biosynthesis pathway by a tri-enzyme system containing LAAD, DAPDH and GDH; (b) Effect of different activity ratio (0.1:1–3:1) of GDH/DAPDH on D-Phe production, with PPA 20 g L⁻¹, NH₄Cl 20 g L⁻¹, glucose 28.0 g L⁻¹ in Tris-HCl buffer (100 mM, pH 9.0, containing NADP⁺ 5 mM). (c) Effect of different activity ratio (0.2:1–3:1) of LAAD/DAPDH on D-Phe production, with L-Phe 20 g L⁻¹, NH₄Cl 4 g L⁻¹, glucose 28.0 g L⁻¹, in Tris-HCl buffer (100 mM, pH 9.0, containing NADP⁺ 5 mM, FAD 5 mM and enough *E. coli* membranes).

In vivo reconstruction of the D-Phe biosynthesis pathway

To construct a highly efficient conversion system for industrial application, three enzymes were designed to co-express in one host cell. Then, the genes PmLAAD, PvDAPDH, and BmGDH were inserted into plasmid pCDFDuet-1 (Figure 2a) and transformed into *Escherichia coli* BL21(DE3), resulting in strain *E. coli* 01. Expression of the three enzymes was verified using SDS-PAGE (Figure S1). The conversion performance of *E. coli* 01 was investigated with 20 g L⁻¹ wet cells at 30 °C (Figure 2c) and 5–25 g L⁻¹ L-Phe. When the L-Phe concentration was increased from 5 g L⁻¹ to 15 g L⁻¹, D-Phe titer increased from 4.2 ± 0.2 g L⁻¹ to 7.2 ± 0.1 g L⁻¹, and the conversion rate decreased from 84.4% to 48.0%. Concurrently, the intermediate PPA increased from 0.5 ± 0.2 g L⁻¹ to 16.2 ± 0.1 g L⁻¹, and it was detected in the transformation broth (Figure S4). This result pointed to inhibition

of the reductive amination reaction catalyzed by PvDAPDH and BmGDH. A comparison of the activities of PmLAAD (40.5 ± 1.0 U g⁻¹), PvDAPDH (8.7 ± 1.3 U g⁻¹), and BmGDH (561.2 ± 6.8 U g⁻¹) revealed a 4.6:1:62 ratio, pointing to PvDAPDH as the bottleneck in this pathway.

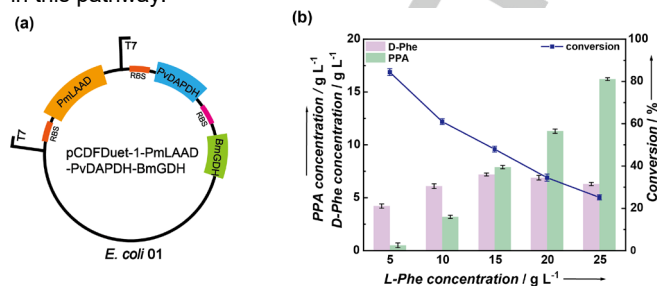


Figure 2. The construction and evaluation of *E. coli* 01. (a) Construction of co-expressed strain *E. coli* 01 with the first T7 promoter followed by PmLAAD, and the second T7 promoter followed by PvDAPDH and BmGDH. (b) The performance of *E. coli* 01 with L-Phe from 5–25 g L⁻¹, *E. coli* 01 whole-cell catalysts 20 g L⁻¹.

Table 1. Activity of PvDAPDH toward other α-keto acids

Substrates	Specific activity (U mg ⁻¹)	ee ^[a]
phenylpyruvic acid	0.08±0.02	99 ^[b]
phenylglyoxylic acid	-	99 ^[b]
2-oxo-4-phenylbutyric acid	0.15±0.02	98 ^[b]
4-hydroxyphenylpyruvic acid	0.05±0.02	99 ^[b]
2-oxobutyric acid	0.03±0.01	98 ^[c]
α-ketovaleric acid	0.03±0.01	97 ^[c]
4-methyl-2-oxopentanoic acid	0.02±0.01	98 ^[c]

[a] The conversions for ee determination were set in 1 mL biotransformation systems containing purified enzyme PvDAPDH 1 U L⁻¹, BmGDH 1 U L⁻¹, α-keto acids 5 g L⁻¹, NH₄Cl 5 g L⁻¹, glucose 7 g L⁻¹ in Tris-HCl buffer (100 mM, pH 9.0), 30 °C for 24 h. [b] The D/L-products were detected by the same analysis method for D/L-Phe. [c] The D/L-products were detected after FDAA-derivatization^[13].

Engineering of PvDAPDH for high catalytic efficiency toward PPA

As shown in Table 1, a study of PvDAPDH substrate specificity revealed low activity toward keto acids including PPA, but high stereospecificity (97–99% ee). To improve the catalytic efficiency of PvDAPDH, a structural model of PvDAPDH was built using StDAPDH (PDB ID: 3WBF)^[18] as template. Docking the cofactor NADPH and imine intermediate 2-imino-3-phenylpropanoic acid in the cofactor-free structure yielded outputs (Figure 3a) whose hydrogen bond interactions in the D-center were almost identical to those with the natural meso-DAP substrate (Figure 3b)^[18–19]. However, a hydride transfer distance of 4.1 Å (3.6 Å reported^[19]) was unfavorable for catalysis. When investigating the L-center, T171 and R181 were found to sterically clash with the benzene ring, thus affecting the binding of bulky substrates. Residue F146 formed a pi-pi interaction with the benzene ring, further pulling the

FULL PAPER

imine center from NADPH and hindering catalysis (Figure 3c). We hypothesized that the poor catalysis toward PPA was determined by tensions on the benzene ring side-chain. Therefore, a "tension release" strategy was proposed, whereby creation of enough space allowed for the binding of bulky substrates and reducing the pulling effect from the L-center facilitated hydride transfer.

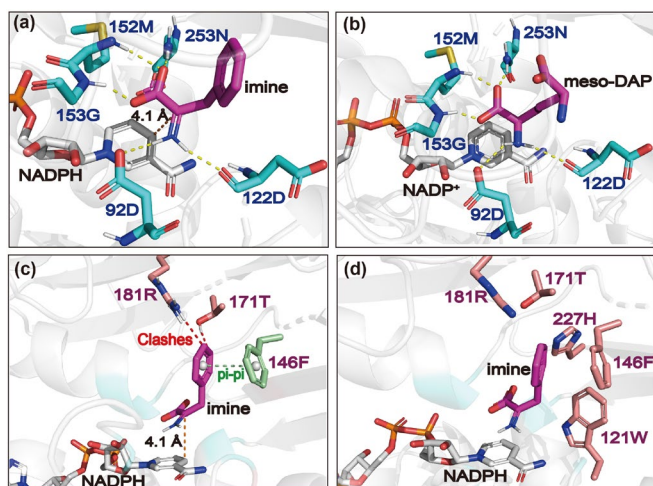


Figure 3. Docking analysis of PvDAPDH. (a) The docking pose in D-center with cofactor NADPH and imine intermediate 2-imino-3-phenylpropanoic acid docked in generated PvDAPDH model; (b) The docking pose of nature substrate meso-DAP in D-center; (c) The interaction of phenyl side-chain in imine intermediate; (d) The selected 5 residues for mutation studies.

Accordingly, five residues in a radius of 5 Å around imine intermediate were selected in the L-center; they included W121, F146, T171, R181, and H227 (Figure 3d). The five selected residues were engineered by semi-saturated mutagenesis using NBT, which contains small residues, and four single variants were obtained (Figure 4a). These included W121A, T171L, R181S, and H227I, whose activities were improved by 15-fold, 8-fold, 9-fold, and 32-fold, respectively. The best single variant, PvDAPDH^{H227I} (2.56 U mg⁻¹), raised the D-Phe titer to 25.4 g L⁻¹. Random recombination of the four single variants yielded a tri-variant, PvDAPDH^{W121A/R181S/H227I}, whose activity of 6.86 U mg⁻¹ was 85-fold higher than in PvDAPDH^{WT}, and it produced 37.8 g L⁻¹ D-Phe (Figure 4a, Figure S8).

Table 2. Kinetic parameters of PvDAPDH^{WT} and its variants toward phenylpyruvic acid

Catalyst	K_M (mM)	k_{cat} (s ⁻¹)	k_{cat}/K_M (s ⁻¹ mM ⁻¹)
PvDAPDH ^{WT}	4.95±1.2	0.19±0.01	0.038
PvDAPDH ^{W121A}	6.19±1.3	2.19±0.22	0.35
PvDAPDH ^{T171L}	6.54±1.9	2.35±0.13	0.35
PvDAPDH ^{R181S}	5.46±1.0	3.73±0.15	0.60
PvDAPDH ^{H227I}	8.3±1.7	8.54±0.52	1.04
PvDAPDH ^{W121A/R181S/H227I}	10.2±2.1	24.8±0.68	2.43

As listed in Table 2, an increase in the k_{cat} and K_M values of the five variants led to a concomitant increase in their k_{cat}/K_M and overall catalytic efficiency. The highest k_{cat}/K_M (2.43 s⁻¹ mM) belonged to PvDAPDH^{W121A/R181S/H227I}, which was chosen for further studies on large α -keto acids, such as phenylbutanoic acid, 4-hydroxyphenylpyruvic acid, and 3-indolylpyruvic acid. As illustrated in Figure 4b, these three keto acids could be converted into the corresponding D-amino acids, with the highest titer of D-homophenylalanine being 38.5 g L⁻¹ and corresponding to a 96.2% conversion rate.

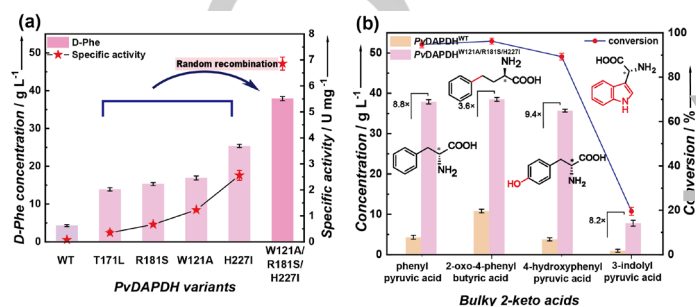


Figure 4. The catalytic efficiency of PvDAPDH variants toward keto-acids. (a) Directed evolution of the parent PvDAPDH^{WT} for reductive amination of PPA; (b) The catalytic efficiency of the PvDAPDH^{W121A/R181S/H227I} toward bulky 2-keto acids. The conversions were performed in 2 mL Tris-HCl buffer (100 mM, pH 9.0, containing 0.5 mM NADP⁺, 40 g L⁻¹ NH₄Cl and 56 g L⁻¹ glucose) with 10 g L⁻¹ PvDAPDH and BmGDH wet whole-cell biocatalysts, 40 g L⁻¹ keto acids, 30°C for 24 h.

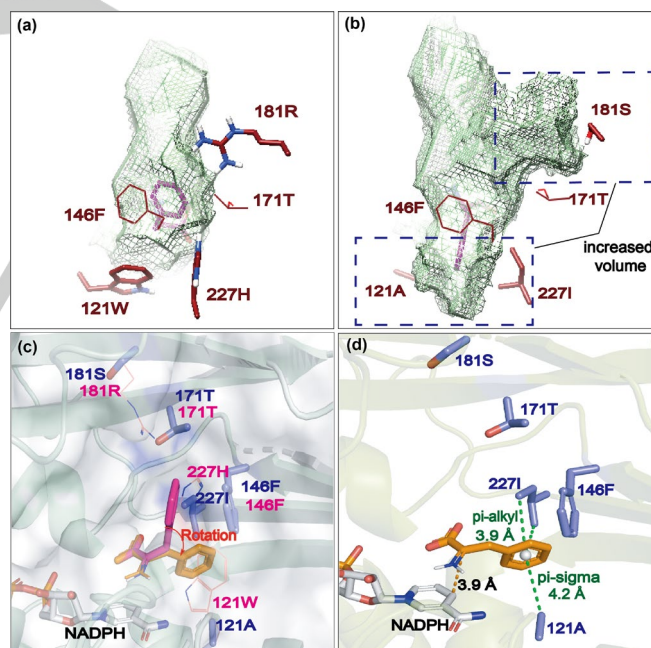


Figure 5. The changes in the binding pocket and interactions of PvDAPDH. (a) The pocket shape of WT; (b) The changed pocket shape and increased volume of variant PvDAPDH^{W121A/R181S/H227I}; (c) Conformation comparison of imine intermediate side-chain in WT (magenta) and in variant PvDAPDH^{W121A/R181S/H227I} (orange); (d) The interaction of imine intermediate and hydride transfer distance in variant PvDAPDH^{W121A/R181S/H227I}.

The catalytic mechanism of the variant DAPDH^{W121A/R181S/H227I} was analyzed from the point of steric hindrance and interactions in the L-center. Spatially, the pocket changed from an elongated cavity to an enlarged one (Figure 5a, 5b), resulting in a 244-Å³

FULL PAPER

increase in pocket volume and the possibility to accommodate the benzene ring. As a result, instead of being projected toward the outside as in the wild-type, the side-chain of the mutant was rotated in such way that it became buried deeply inside the pocket (Figure 5c). Accordingly, the pi-pi interaction of the benzene ring with F146 was replaced by a weaker pi-alkyl interaction with W121A and a pi-sigma interaction with H227I (Figure 5d). These changes allowed the side-chain to release tension and meanwhile shortened the hydride transfer distance by 0.2 Å (from 4.1 Å to 3.9 Å), allowing the imine intermediate easier access to NADPH (Figure 5d). The disappeared pi-pi interaction in the L-center might account for the increased K_M (from 4.95 mM to 10.2 mM), which was in line with the calculated increase in binding energy from -7.5 kcal mol⁻¹ to -7.1 kcal mol⁻¹. The enlarged binding pocket and reduced hydride transfer distance greatly elevated the k_{cat} (by 130-fold) and k_{cat}/K_M (64-fold). In practice, the reshaped pocket space and reduced hydride transfer distance were responsible for improving the catalytic efficiency of PvdDAPDH^{W121A/R181S/H227I}.

One-pot production of D-Phe through a tri-enzymatic cascade

PvdDAPDH was replaced by PvdDAPDH^{W121A/R181S/H227I} in *E. coli* 01. The resulting strain, *E. coli* 02, generated 35.6 g L⁻¹ D-Phe at 40 g L⁻¹ L-Phe and 20 g L⁻¹ wet cells (Figure 6a). However, 3.8 g L⁻¹ L-Phe remained in the transformation broth and no PPA intermediate was detected. This could be explained by PmLAAD, PvdDAPDH, and BmGDH in *E. coli* 02 having an activity of 42.3 ± 1.2 U g⁻¹, 120.8 ± 1.9 U g⁻¹, and 532.3 ± 4.5 U g⁻¹, respectively,

corresponding to an enzymatic activity ratio of 0.35:1:4.4; therefore, PmLAAD acted as the limiting step. To overcome this bottleneck, PmLAAD gene copy number was increased to two (*E. coli* 03) and three (*E. coli* 04) copies. PmLAAD activity increased to 58.4 ± 1.3 U g⁻¹ in *E. coli* 03, bringing the PmLAAD:PvdDAPDH:BmGDH activity ratio to 0.57:1:3.1 (Figure 6b), which closely resembled the in vitro reconstruction result. Whole-cell catalysis in *E. coli* 03 produced, 38.7 g L⁻¹ D-Phe from 40 g L⁻¹ L-Phe, corresponding to a 96.8% conversion rate, and without any L-Phe and PPA in the transformation broth (Figure 5d). Interestingly, D-Phe titer and conversion were lower in *E. coli* 04 than in *E. coli* 03. It seems that duplication of LAAD gene improved its activity meanwhile it also affected the expression of DAPDH and GDH, making DAPDH insufficient for further conversion (Figure S2).

The effect of substrate feeding, buffer pH (7.5 to 9.5), and temperature (20 to 37°C) on D-Phe titer were investigated at 100-mL scale with 60 g L⁻¹ L-Phe. As shown in Figure 7a, use of 20 g L⁻¹ wet *E. coli* 03 for whole-cell catalysis yielded 54.2 ± 1.3 g L⁻¹ D-Phe, amounting to a conversion rate of 90.3% when L-Phe was fed at 10 g L⁻¹ every 2 h together with 2 g L⁻¹ NH₄Cl and 14 g L⁻¹ glucose. Increasing the pH of the Tris-HCl buffer to 8.5 pushed the D-Phe titer to 56.1 ± 1.2 g L⁻¹ (Figure 7b). Finally, as shown in Figure 7c, D-Phe titer (57.4 ± 1.4 g L⁻¹) and conversion yield (95.7%) were highest at a temperature of 25°C. Thus, optimum transformation conditions (20 g L⁻¹ wet *E. coli* 03, pH 8.5, 100 mM Tris-HCl, 25°C), resulted in 57.8 ± 1.1 g L⁻¹ D-Phe from 60 g L⁻¹ L-Phe during 30 h in a 3-L fermentor, corresponding to 96.3% conversion rate and >99% ee.

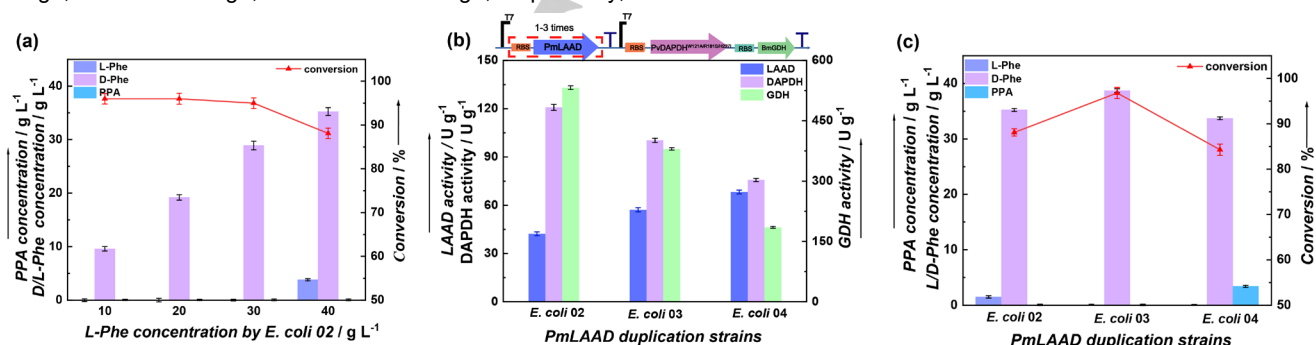


Figure 6. Optimization of PmLAAD in co-expressed strain by different copies. (a) D-Phe production by strain *E. coli* 02 with L-Phe 40 g L⁻¹ and wet whole-cell biocatalysts 20 g L⁻¹ in 10 mL Tris-HCl buffer (100 mM, pH 9.0, containing 0.5 mM NADP⁺, 8 g L⁻¹ NH₄Cl and 56 g L⁻¹ glucose), 30°C for 30 h; (b) The assay of activity in co-expressed strain with different copies of PmLAAD. (c) Effect of different PmLAAD copies on D-Phe production with L-Phe 40 g L⁻¹ and wet whole-cell biocatalysts 20 g L⁻¹, in 10 mL Tris-HCl buffer (100 mM, pH 9.0, containing 0.5 mM NADP⁺, 8 g L⁻¹ NH₄Cl and 56 g L⁻¹ glucose), 30°C for 30 h.

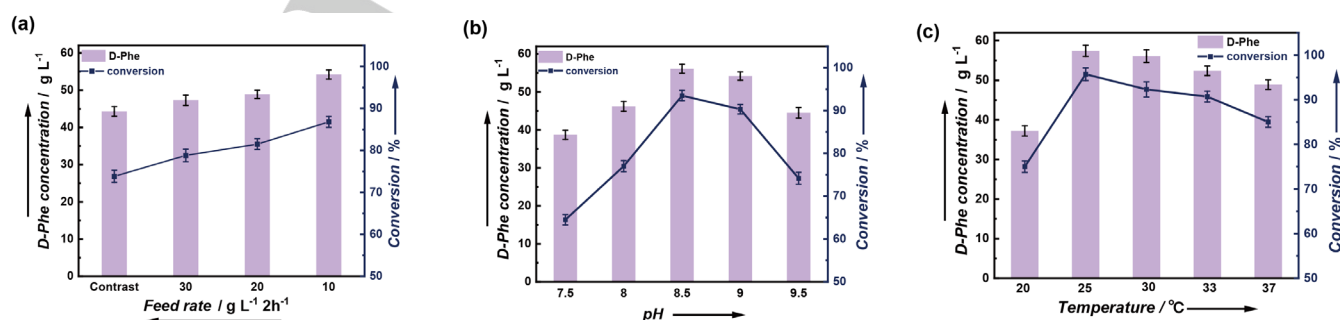


Figure 7. Optimization of conversion process by strain *E. coli* 03. (a) Effect of feed rate of L-Phe on D-Phe concentration; (b) Effect of conversion pH on D-Phe concentration; (c) Effect of conversion temperature on D-Phe concentration. The conversion reactions were performed in a 100 mL volume of 100 mM Tris-HCl buffer, containing NADP⁺ 0.5 mM, with wet whole-cell biocatalysts, 20 g L⁻¹, NH₄Cl 12 g L⁻¹ and glucose 84 g L⁻¹, for 30 h.

FULL PAPER

Discussion

The aim of the present study was to develop a highly efficient method for the production of D-Phe. To this end, a tri-enzymatic cascade, which included PmLAAD, PvDAPDH, BmGDH, and L-Phe as substrate, was designed and reconstructed *in vivo*. The efficiency of this cascade was further improved by increasing the catalytic activity of PvDAPDH (6.86 U mg⁻¹) up to 85-fold toward PPA, a limiting step in the cascade. Use of a “tension release” strategy led to the best PvDAPDH variant, PvDAPDH^{W121A/R181S/H227I}, which achieved one-pot conversion of L-Phe to 57.8 g L⁻¹ D-Phe, with 99% ee in 30 h at a 3-L scale. These values are suitable for industrial-scale production of D-Phe from a cheap amino acid source such as L-Phe.

The enzymatic cascade described here represents a chiral reset process with PPA as intermediate. It benefits from the low price of substrate (L-Phe) and elevated enantioselectivity. Various enzymatic methods have been developed to synthesize D-Phe: (1) In the hydantoinase process, racemic 5-benzylhydantoin acts as substrate (Figure 8a) for a cascade that involves hydantoin racemase, D-hydantoinase, and N-carbamoyl-D-amino acid amidohydrolase. D-Phe is produced at high yield (45.9 g L⁻¹, 98% molar yield) and 99% enantioselectivity in 48 h^[3b]; however, the low solubility of substrate represents a rate-limiting step and leads to prolonged conversion times^[20]. (2) In transamination processes, PPA and D-glutamate act as co-substrates (Figure 8b), with PPA being transaminated to D-Phe via D-transaminase, while D-glutamate is converted to α-ketoglutarate. During this catalytic process, NAD⁺ and formate are fed to the transformation broth to provide enough NADH. Glutamate dehydrogenase and glutamate racemase help recycle α-ketoglutarate back to D-glutamate, while FDH restores the reducing power (NADH). This process has yielded 58 g L⁻¹ D-Phe with 100% ee in 35 h^[4b]. (3) Asymmetric resolution processes utilize D/L-Phe as substrate and phenylalanine ammonia-lyase for the resolution from racemate^[21] (Figure 8c). Although enantioselectivity can be quite high (>99%), the conversion rate of this process is limited to 50%, making downstream purification more difficult^[5b].

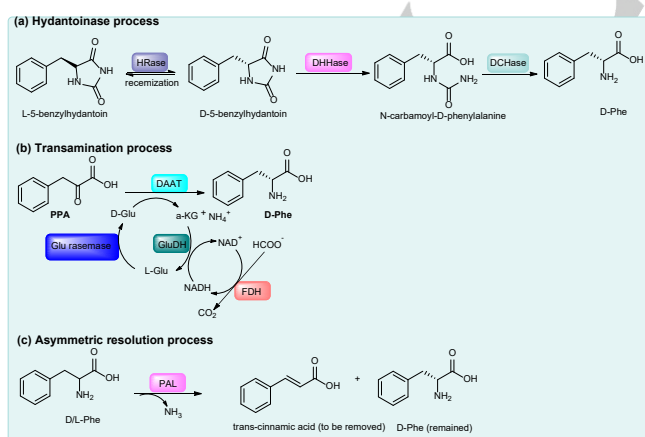


Figure 8. Three other ways to produce D-Phe. (a) Hydantoinase process; (b) Transamination process; (c) Asymmetric resolution process.

DAPDH is an excellent enzyme to convert bulky aromatic α-keto acids to the corresponding D-amino acids. The catalytic activity and substrate specificity of DAPDH toward bulky aromatic α-keto acids has been a potential bottleneck in industrial applications. In this study, the low activity of PvDAPDH toward PPA was the limiting step for efficient D-Phe production. A “tension release” strategy in the L-center was proposed and led to PvDAPDH^{W121A/R181S/H227I}, an improved variant with 85-fold increased specific activity and 64-fold increased k_{cat}/K_M . During the past decade, various rational protein engineering strategies based on the analysis of structure–function relationships or catalytic mechanisms have been used to increase the catalytic efficiency of DAPDH. A double-site variant, StDAPDH^{W121L/H227I}, was achieved through structure-guided pocket engineering. Compared with wild-type StDAPDH, the activity of StDAPDH^{W121L/H227I} toward 2-oxo-4-phenylbutyric acid was increased by 34-fold^[13]. Substrate specificity of DAPDH could also be broadened. For example, DAPDH from *Clostridium tetani* E88 was mutated to CtDAPDH^{Q154L/T173I/R199M/P248S/H249N/N276S}, which caused the activity toward PPA to increase from 0 to 0.11 U mg⁻¹^[22]. Here, analysis of steric hindrance and unfavorable interactions, whereby increased molecular tension and decreased the catalytic activity, identified five candidate residues for semi-saturation mutagenesis. The best resulting variant, PvDAPDH^{W121A/R181S/H227I}, had an expanded binding pocket, allowing the PPA side-chain to be rotated and buried further in the cavity of PvDAPDH, thus releasing the tension and shortened the hydride transfer distance.

By introducing variant PvDAPDH^{W121A/R181S/H227I} into *E. coli* 03 and then optimizing transformation conditions, 57.8 g L⁻¹ D-Phe was achieved with 96.3% conversion and >99% ee via a one-pot transformation. A similar study combining PmLAAD whole-cell with purified StDAPDH^{H227V} and *Burkholderia stabilis* BsFDH yielded 13.2 g L⁻¹ D-Phe in 6 h, with 100% conversion rate and >99% ee^[15]. And more recently, the three enzymes were assembled in one cell and the titer of D-Phe was improved to 24.7 g L⁻¹ in 24 h by 75 g L⁻¹ whole-cell catalyst and 15 mM NADP⁺^[23]. A quick cost analysis of our final process from materials and catalyst showed that the cost for D-Phe production is about \$11450 per ton. By contrast, the factory price for D-Phe is as high as \$30500 per ton (Table S4). Therefore, the cascade pathway developed in this study greatly improves previous D-Phe titers and provides an attractive strategy for the industrial production of D-Phe.

Experimental Section

Materials

The expression plasmid pET-28a(+), pCDFDuet-1 and the host strain *E. coli* BL21(DE3) were purchased from Novagen (Madison, WI, USA). PmLAAD variant (patent application number: 202011588760.0) and BmGDH (UniProtKB: A7XZE6_BACME) were reserved by our Lab. PvDAPDH (NCBI: WP_075674287.1) was cloned from *Proteus vulgaris*. Other DAPDH genes were cloned from corresponding strains (Table S1). The restriction

FULL PAPER

enzymes (*Bam*HI, *Nco*I, *Eco*RI, *Hind*III, *Not*I, *Nde*I, *Xho*I, *Kpn*I, and *Dpn*I), primerSTAR polymerase, T4 Ligase, plasmid miniprep kit, agarose gel DNA purification kit were supplied by TaKaRa (Dalian, China) and one step cloning kit was supplied by Vazyme (Nanjing, China). All other chemicals and solvents were obtained commercially.

Molecular modeling

The 3D structural models of PvDAPDH and its mutant were constructed based on X-ray crystal structure of the StDAPDH from *Symbiobacterium thermophilum* (PDB ID: 3WBF) by homology modeling (<https://swissmodel.expasy.org/>). Cofactor NADPH/ NADP⁺ was first docked into PvDAPDH to obtain the binary complex by Auto Dock Vina, then the imine intermediate 2-imino-3-phenylpropanoic acid or nature substrate meso-diaminopimelate was further docked into the binding site. The pocket volume was calculated by binding site detection website (<https://proteins.plus/>).

Construction of the co-expressed strains

Main primers used for constructing co-expressed strains were summarized in Table S3. PmLAAD gene was firstly inserted into pCDFDuet-1 after the first T7 promoter using restriction sites *Bam*HI and *Hind*III. Gene duplication of PmLAAD (added with RBS sequence) was further inserted by restriction sites *Hind*III (2 copies) and *Not*I (3 copies). Then PvDAPDH gene was inserted after the second promoter using the restriction sites *Nde*I and *Kpn*I, followed by BmGDH gene (added with RBS sequence, by restriction sites *Kpn*I and *Xho*I).

Mutant library construction and screening

The primers used for constructing PvDAPDH and its variants were summarized in Table S2. PvDAPDH (WP-0756742847.1) from *Proteus vulgare* was inserted into the pET-28a (+) using the restriction sites *Nco*I and *Eco*RI for expression in *E. coli* BL21 (DE3). Semi-saturation mutagenesis and the recombination of variants were carried by whole plasmid PCR protocol (PrimeSTAR) and the PCR product was digested by *Dpn*I and then transformed into *E. coli* BL21 (DE3) cells for further screening and DNA sequencing (Genewiz, China). To high-efficiently screen the positive variant from 96-well plate, the supernatants were prepared and used for activity screening by monitoring the NADPH consumption at 30°C in a reaction system of Tris-HCl buffer (100 mM, pH 9.0), containing 160 µL crude enzyme extract, 20 µL substrate mixture (200 mM PPA and 2 M NH₄Cl), and 20 µL of NADPH (10 mM). Variants with 3-fold higher activity toward PPA than wild-type enzyme were selected.

Analytical methods

D-Phe and L-Phe levels were determined by high-performance liquid chromatography (HPLC) using a VWD detector with a CrownPak CR(+) column (4×150 mm, 5 µm), eluted with HClO₄

(pH 1.5):acetonitrile (8:2) at a flow rate of 0.2 mL min⁻¹ (25°C) and detected at 210 nm. Samples for D/L-Phe detection were first dissolved in 2M NaOH and then centrifuged at 12,000 × g for 20 min. The supernatant was then diluted by HClO₄ (pH 1.5) and filtered using 0.22-µm filter membrane. The concentration of PPA was also detected by HPLC. The samples for PPA detection were centrifuged and filtered through 0.22-µm filter membrane. Samples were separated by Bio-Rad Aminex HPX-87H column (300×7.8 mm, 9 µm), eluted with 0.005 M H₂SO₄ (0.6 mL min⁻¹, 35°C) and detected at 210 nm.

Enzyme expression and purification

PmLAAD, PvDAPDH and BmGDH were individually overexpressed and purified from *E. coli* BL21(DE3) with pET28a(+) plasmid (Table S2). Cells were harvested by centrifugation at 6,000 × g for 10 min and resuspended in Tris-HCl buffer. The cell suspensions were ruptured by high pressure cell crusher at 4°C and centrifuged at 12,000 × g for 20 min. The recombinant strains were purified by an AKTA pure system (GE Healthcare Life Science, USA) with a nickel-affinity column (for PmLAAD and BmGDH) and anion exchange column (for PvDAPDH).

Enzyme assay

PmLAAD (EC: 1.4.3.2) activity on L-Phe was assayed by coupling PPA formation. The reaction system (Tris-HCl buffer, 100 mM, pH 9.0, 30°C) contained 20 g L⁻¹ L-Phe. One unit of PmLAAD activity (U) was calculated as the amount of enzyme producing 1 µmol of PPA in 1 min. PvDAPDH (EC: 1.4.1.16) activity on PPA was assayed by coupling NADPH consumption. The reaction system contained 50 mM PPA, 200 mM NH₄Cl and 2 mM NADPH. One unit of PvDAPDH activity (U) was calculated as the amount of enzyme consuming 1 µmol of NADPH in 1 min. BmGDH (EC: 1.1.1.47) activity on glucose was assayed by coupling NADPH formation. The reaction system contained 50 mM glucose, 2 mM NADP⁺. One unit of BmGDH activity (U) was calculated as the amount of enzyme producing 1 µmol of NADPH in 1 min. The activity of the recombinant strains expressed single enzyme was measured using purified enzyme, while the activity of the co-expressed strains was measured using wet whole-cell catalysts (for PmLAAD) and the supernatant (for PvDAPDH and BmGDH).

Determination of kinetic parameters

Kinetic parameters for reductive amination of PPA were performed at 30°C in Tris-HCl buffer (100 mM, pH 9.0), which contained NH₄Cl 200 mM, NADPH 2 mM, with PPA concentration varied from 2 to 50 mM. DAPDH was added to start the reaction, and the absorbance in 340 nm were monitored in the process. All of the experiments were conducted with three replicates. *K_M* and *k_{cat}* were calculated by nonlinear fitting by Origin software.

Production of D-Phe from L-Phe

FULL PAPER

The strains were harvested by centrifugation at 6,000 × g for 10 min after overexpression. The conversion experiments were carried out in a 3-L bioreactor with 1-L working volume. Substrates L-Phe, NH₄Cl and glucose were fed to the reaction system every 2 h. Because the cascade reactions by BmGDH was pH-decreasing, in a 3-L reactor, 2 M NaOH was used to control pH automatically. The concentration of D-Phe, L-Phe, and phenylpyruvic acid was determined using the HPLC method as described above.

Isolation Protocols

The D-Phe product in reaction mixture was isolated using a Dowex 50WX8 cation exchange column. First, the resin was washed in sequence by NH₄OH (2 M, 2×30 ml), HCl (2 M, 2×30 ml) and H₂O (4×30 mL). Then, the reaction mixture (centrifuged) was acidified with 1 M HCl and loaded onto the column. Finally, the column was washed with HCl (1M, 2×30 mL), H₂O (4×30 mL) and eluted with NH₄OH (2 M, 4×30 mL). Fractions containing D-Phe were combined and lyophilized to remove the water, and then purified by preparation thin liquid chromatography (PTLC) with developing solvent: n-BuOH/H₂O/HOAc(4:1:1). Silica gel containing target amino acid was collected and eluted with n-BuOH/H₂O (2:1). After filtration, the organic solvent was evaporated by nitrogen blowing, and the product was dried overnight under vacuum. The solid was washed with (EtOH/H₂O, 9:1) to afford D-amino acids in high chemical purity.

Data availability

All of the mutants described in this manuscript are available from the corresponding author upon request.

Acknowledgements

This work was financially supported by the National Natural Science Foundation of China (grant numbers: 22008089 and 21878126), Provincial Natural Science Foundation of Jiangsu Province (grant number: BK20200622), the key technologies R & D Program of Jiangsu Province (grant number: BE2018623), and the National First-Class Discipline Program of Light Industry Technology and Engineering (grant number: LITE2018-20).

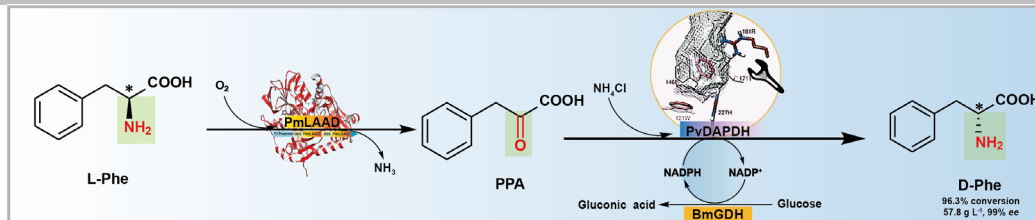
Keywords: D-phenylalanine • DAPDH • enzyme cascade • catalytic efficiency • tension release

- [1] a) M. Friedman, *Chem. Biodiversity* **2010**, *7*, 1491-1529; b) J. Liu, J. Liu, L. Chu, Y. Zhang, H. Xu, D. Kong, Z. Yang, C. Yang, D. Ding, *ACS Appl. Mater. Interfaces* **2014**, *6*, 5558-5565; c) M. Munoz, S. Recio, M. Rosso, M. Redondo, R. Covenas, *J. Physiol. Pharmacol.* **2015**, *66*, 421-426; d) E. Başaran, A. Karaküçük-Lyidoğan, D. Schols, E. E. Oruç-Emre, *Chirality* **2016**, *28*, 495-513.
- [2] a) Y.-P. Xue, C.-H. Cao, Y.-G. Zheng, *Chem. Soc. Rev.* **2018**, *47*, 1516-1561; b) L. Pollegioni, E. Rosini, G. Molla, *Int. J. Mol. Sci.* **2020**, *21*, 3206.
- [3] a) H. B. Dae, J. J. Song, S.-G. Lee, S. J. Kwon, Y. Asano, M.-H. Sung, *Enzyme Microb. Technol.* **2003**, *32*, 131-139; b) H. Nozaki, Y. Takenaka, I. Kira, K. Watanabe, K. Yokozeki, *J. Mol. Catal. B: Enzym.* **2005**, *32*, 213-218; c) J. M. Clemente-Jiménez, S. Martínez-Rodríguez, F. Rodríguez-Vico, F. J. L. Heras-Vázquez, *Recent Pat. Biotechnol.* **2008**, *2*, 35-46.
- [4] a) A. Galkin, L. Kulakova, H. Yamamoto, K. Tanizawa, H. Tanaka, N. Esaki, K. Soda, *J. Ferment. Bioeng.* **1997**, *83*, 299-300; b) H.-S. Bae, S.-P. Hong, S.-G. Lee, M.-S. Kwak, N. Esaki, M.-H. Sung, *J. Mol. Catal. B: Enzym.* **2002**, *17*, 223-233; c) H.-S. Bae, S.-G. Lee, S.-P. Hong, M.-S. Kwak, N. Esaki, K. Soda, M.-H. Sung, *J. Mol. Catal. B: Enzym.* **1999**, *6*, 241-247; d) H. Zhou, L. Meng, X. Yin, Y. Liu, G. Xu, J. Wu, M. Wu, L. Yang, *Eur. J. Org. Chem.* **2019**, *38*, 6470-6477.
- [5] a) L. Zhu, L. Zhou, N. Huang, W. Cui, Z. Liu, K. Xiao, Z. Zhou, *PLoS One* **2014**, *9*, e108586; b) F. Parmeggiani, N. J. Weise, S. T. Ahmed, N. J. Turner, *Chem. Rev.* **2018**, *118*, 73-118.
- [6] K. Vedha-Peters, M. Gunawardana, J. D. Rozzell, S. J. Novick, *J. Am. Chem. Soc.* **2006**, *128*, 10923-10929.
- [7] H. Misono, H. Togawa, T. Yamamoto, K. Soda, *J. Bacteriol.* **1979**, *137*, 22-27.
- [8] a) H. Misono, M. Ogasawara, S. Nagasaki, *Agric. Biol. Chem.* **1986**, *50*, 2729-2734; b) H. Misono, H. Togawa, T. Yamamoto, K. Soda, *Biochem. Biophys. Res. Commun.* **1976**, *72*, 89-93.
- [9] X. Gao, Z. Zhang, Y. n. Zhang, Y. Li, H. Zhu, S. Wang, C. Li, *Appl. Environ. Microbiol.* **2017**, *83*, e00476-17.
- [10] a) S. G. Reddy, G. Scapin, J. S. Blanchard, *Proteins: Struct., Funct., Genet.* **1996**, *25*, 514-516; b) G. Scapin, S. G. Reddy, J. S. Blanchard, *Biochemistry* **1996**, *35*, 13540-13551.
- [11] X. Gao, X. Chen, W. Liu, J. Feng, Q. Wu, L. Hua, D. Zhu, *Appl. Environ. Microbiol.* **2012**, *78*, 8595-8600.
- [12] a) H. Akita, Y. Nakamichi, T. Morita, A. Matsushika, *Microbiologyopen* **2020**, e1059; b) H. Akita, Y. Nakamichi, T. Morita, A. Matsushika, *Biochim. Biophys. Acta, Proteins Proteomics* **2020**, *1868*, 140476.
- [13] X. Cheng, X. Chen, J. Feng, Q. Wu, D. Zhu, *Catal. Sci. Technol.* **2018**, *8*, 4994-5002.
- [14] F. Parmeggiani, S. T. Ahmed, M. P. Thompson, N. J. Weise, J. L. Galman, D. Gahloth, M. S. Dunstan, D. Leys, N. J. Turner, *Adv. Synth. Catal.* **2016**, *358*, 3298-3306.
- [15] D. Zhang, X. Jing, W. Zhang, Y. Nie, Y. Xu, *RSC Adv.* **2019**, *9*, 29927-29935.
- [16] L. Zhao, W. Liu, X. Chen, M. Wang, J. Feng, Q. Wu, D. Zhu, *Chin. J. Biotechnol.* **2015**, *31*, 1108-1118.
- [17] J. Li, J. Pan, J. Zhang, J.-H. Xu, *J. Mol. Catal. B: Enzym.* **2014**, *105*, 11-17.
- [18] W. Liu, Z. Li, C.-H. Huang, R.-T. Guo, L. M. Zhao, D. Zhang, X. Chen, Q. Wu, D. Zhu, *Chembiochem* **2014**, *15*, 217-222.
- [19] X. Gao, F. Huang, J. Feng, X. Chen, H. Zhang, Z. Wang, Q. Wu, D. Zhu, *Appl. Environ. Microbiol.* **2013**, *79*, 5078-5081.
- [20] S.-F. Wang, Y. Huang, F.-Y. Liao, H.-Y. Zeng, G. Xu, *Chem. Eng. Des. Commun.* **2019**, *45*, 164-165.
- [21] Y.-Q. Fang, L.-B. Zhu, N. Huang, L. Zhou, Z.-Y. Ding, Y. Liu, Z.-M. Zhou, *Sci. Technol. Food Ind.* **2015**, *36*, 243-246.
- [22] W. Liu, R.-T. Guo, X. Chen, Z. Li, X. Gao, C.-H. Huang, Q. Wu, J. Feng, D. Zhu, *ChemBioChem* **2015**, *16*, 924-929.
- [23] D.-P. Zhang, X.-R. Jing, L.-J. Wu, A.-W. Fan, Y. Nie, Y. Xu, *Microb. Cell Fact.* **2021**, *20*, 11.

FULL PAPER

Entry for the Table of Contents

FULL PAPER



D-Phe is an important intermediate in food and pharmacy. In this study, we constructed a tri-enzymatic cascade reaction for the generation of D-Phe from cheap L-Phe, employing the enzymes LAAD, DAPDH and GDH. Limited by poor catalytic efficiency of DAPDH, PPA intermediate was found accumulated when producing D-Phe in whole-cell system. We improved its activity towards PPA by protein engineering. By integrating the best DAPDH variants into the system and further duplication of the LAAD gene, we approached to the optimal activity ratio among LAAD, DAPDH and GDH and realized high production of D-Phe.